Journal of Cleaner Production 205 (2018) 313–328

Contents lists available at ScienceDirect

Journal of Cleaner Production

journal homepage: www.elsevier.com/locate/jclepro

Future scenarios of land-use suitability modeling for agricultural sustainability in a river basin

Satiprasad Sahoo [a, *], Indrani Sil [b], Anirban Dhar [c], Anupam Debsarkar [d], Pulakesh Das [e], Amlanjyoti Kar [f]

[a] Faculty of Interdisciplinary Studies, Law & Management, Jadavpur University, Kolkata, India
[b] Department of Remote Sensing & GIS, Vidyasagar University, India
[c] Department of Civil Engineering, IIT Kharagpur, Kharagpur, India
[d] Department of Civil Engineering, Jadavpur University, Kolkata, India
[e] Center for Oceans, Rivers, Atmosphere and Land Science, IIT Kharagpur, Kharagpur, India
[f] Central Ground Water Board, Kolkata, India

ARTICLE INFO

Article history:
Received 14 April 2018
Received in revised form
2 August 2018
Accepted 11 September 2018
Available online 15 September 2018

Keywords:
Land suitability zones
AHP
LULC change
Climate change
Dyna-CLUE
SDSM

ABSTRACT

The present study focuses on future scenarios of land-use suitability zone (LSZ) mapping based on the analytic hierarchy process (AHP) for agricultural sustainability. Proposed case study area is Dwarakeswar - Gandheswari river basin, India. Future estimation of LULC and climate scenarios has been performed. Dynamic Conversion of Land-Use and its Effects (Dyna-CLUE) model and Statistical DownScaling Model (SDSM) are used for this analysis. CLUE model performs the dynamic simulation of land use conversion based on competition between land uses. Future LULC maps are utilized for LSZs mapping. Future LULC scenarios are developed starting from the year 1990. Various hydro-meteorological and geological parameters (Elevation, slope, rainfall, soil, geology, future LULC, groundwater level, evapotranspiration (ET), soil moisture and NDVI) are considered for LSZs. Overall LULC classification accuracy of 1990, 2000 and 2010 is 94.29%, 95.70% and 95%. The LSZs (poor, moderate, good, very good and unsuitable) are evaluated with four scenarios (for the years 2010, 2030, 2050 and 2080). The results reveal a maximum conversion of cultivated land to urban built-up land. The accuracy of the predictive LULC model is tested using receiver operating characteristic (ROC: Built-up- 0.985) curves. Moreover, the unsuitable zones for agricultural sustainability are on the downstream portion of the river basin. Finally, LSZs are validated by using 20 soil moisture field sample points in the proposed command area. These analyses provide valuable information to land use planners for taking a preliminary decision.

1. Introduction

India is bestowed with valuable natural resources consisting of forests, mineral deposits, wetlands, rivers, surface water bodies and vast areas of agricultural serving the needs of around a billion population and varied ecological functions. Due to increase in population, industrialization and with large variations in climate and natural disasters, the natural resources management has become very complex (Hoeppe, 2016). The present land use system shows that there is a very few landscapes which belong to their original state. This land use system plays a key role in establishing a link between the biosphere and the socioeconomic structure. Anthropogenic factors have significantly altered the land use and with the passage of time man is leaving behind a profound change in the environment which is ultimately resulting in an observable changed pattern of land use over time. Observational and modeling studies involving the presence (or absence) of large dams and their associated LULC change should be the key to understanding how the historical impact of dams on climate will play out in the future for better dam building and operations. Water management requires a good understanding of the geographical and spatial information (e.g., rainfall, temperature, Land use/cover, soil, geology, elevation, and watershed). Dwarakeswar-Gandheswari river basin is a water-scarce basin. It is proposed that two reservoirs will be constructed on Dwarakeswar and Gandheswari rivers respectively. Upon construction, farmers will be able to utilize the water from

* Corresponding author. Faculty of Interdisciplinary Studies, Law & Management Jadavpur University Kolkata WB 700032 India.
E-mail address: satispss@gmail.com (S. Sahoo).

https://doi.org/10.1016/j.jclepro.2018.09.099

the canal irrigation system. The command area development is focused on the development of an effective water management system. Water Resources Information System (WRIS, INDIA) does not provide information about this relatively small watershed. Thus a sustainable, integrated water management plan is required for the Dwarakeswar-Gandheswari river basin. In the present work, a methodology is proposed for the future changes in LSZs in Dwarakeswar-Gandheswari river basin.

Few pieces of research are available for future prediction of LULC changes using the Dyna – CLUE model. No attempt has been made to model future scenarios of land suitability zone based on AHP using GIS platform. A multi-model framework for simulating multiple biotic and abiotic factors, including land-use and climate change is available in McRae et al. (2008). Lourdes et al. (2011) applied eleven driving factors for a dynamic land cover simulation model based on Dyna-CLUE since 1997 to 2005 using logit regression models in Dulce Creek basin. Sun et al. (2012) studied the spatial pattern of LULC changes using (surface modeling of land cover change (SMLC) in China. Choudhari (2013) researched on uncertainty modeling for asynchronous time series data with the incorporation of spatial variation for LULC change in the Upper Ganga Basin area. Le Roux (2012) quantified the spatial implications of future land use policies in South Africa through land use modeling. Igbokwe et al. (2013) analyzed LULC for a sustainable development using high-resolution satellite images and GIS in the Onitsha urban and its environs in southeastern Nigeria. Elsheikh et al. (2013) studied agricultural land suitability zone mapping for tropical and subtropical crops based on Geo-environmental factors. Promper et al. (2014) analyzed landslide risk development over time by analyzing the past land cover, as well as modeling potential future scenarios. Scenario simulators and the prediction of LULC changes are available in Han et al. (2015) in Beijing, China. Yalew et al. (2016) analyzed LSZ for agricultural using remote sensing, GIS and AHP techniques in the Abbay basin. Aquilue et al. (2017) used three parameters to assess the change of Cataltonia in the Mediterranean region and his results focused on the spatial drivers of land-cover occurrence to the processes of change emergence and expansion. Li et al. (2017a, b) studied the interaction between land use/cover change (LUCC) and the regional climate change in an arid grassland ecosystem of Inner Mongolia, China. Amici et al. (2017) performed a change detection analysis of LULC mapping based on the multi-temporal approach in MaxEnt modeling. Qiu et al. (2017) studied land use, suitability analysis based on AHP for livestock development planning in the Hangzhou metropolitan area, China.

Steiner (2004) established ecological design, human ecology, national and global environmental archive for the future framework. Population dynamics, consumption, urban, regional and global environmental process drivers influence to change landscapes. Various studies are available with the ideal point method (IPM), ordered weighted averaging (OWA), weighted linear combination (WLC), weighted potential-constraint method for land suitability zone mapping (Liu et al., 2014; Qiu et al., 2017). Most of the methods depend on a huge number of input parameters excluding AHP. AHP is a structured technique for complex decision making. It depends on the theory of prioritization (Saaty, 2005). Moreover, AHP is a comprehensive and rational framework for a decision problem and evaluating alternative solutions. In the present research, an AHP based new land suitability index (LSI) modeling framework is utilized for the rigorous analysis of potential sustainable water resources management. Dyna -CLUE, a dynamic land cover simulation model, is utilized for simulation of future LULC change scenarios. SDSM model is used for deriving future climate change scenarios. Thirteen features (Aspect, elevation, slope, rainfall, temperature, soil depth, geology, distance from the road, distance from the rail, distance from the river, distance from built-up, distance from cropland, distance from forest cover) are utilized for future estimation of LULC. Accuracy assessment is performed based on Google earth images. Also, field verification has been performed in the proposed command area. All the features are developed in remote sensing and GIS environments.

2. Methodology

2.1. Case study description

Dwarakeswar River is a major river in the western part of West Bengal in India (Fig. 1). Dwarakeswar River is also known as Dhalkishore (Annual Flood Report for the Year of 2014, Irrigation &

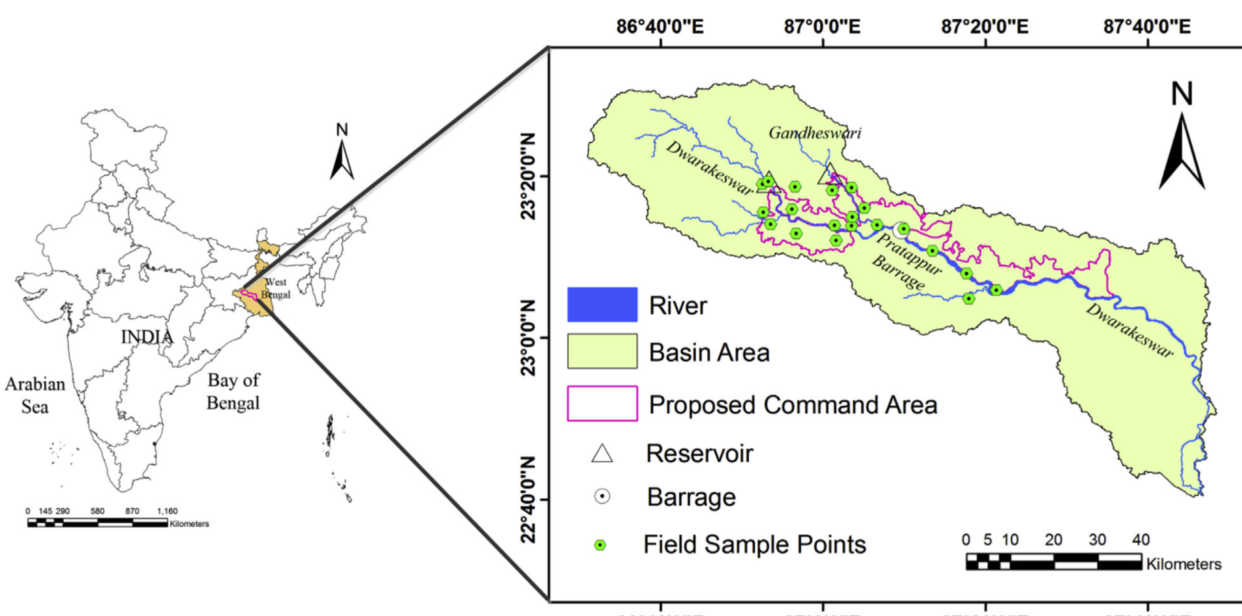

Fig. 1. Location map of the study area.

Waterways Directorate, West Bengal). The river begins from a Tilboni hill in Purulia district and comes Bankura district near Chhatn. Gandheswari River is the main tributary of the Dwarakeswar River. Gandheswari River rises from the district of Bankura and meets of the Dwarakeswar River near Bankura town. Dwarakeswar-Gandheswari river basin area spans from the latitude of 22°37′ to 23°33′N and longitudes of 86°31′ to 87°51′E, approximately covering an area of 4341.765 Km^2. The proposed command area is in the District of Bankura and is bounded by the right bank of river Damodar in the north and north-eastern side and by the left bank of river Dwarakeswar in the south and south-western side. Proposed Dwarakeswar Dam site (23°19′24″ N; 86°53′20″ E), Gandheswari Dam site (23°20′26″ N; 87°00′52″" E), and Barrage (23°13′20″ N; 87°09′39″ E) are situated in Bankura district of West Bengal (EIA-EMP-Report for the Year of 2007, Irrigation & Waterways Directorate, Government of West Bengal). Lateritic soils are present in the western part in the districts of Bankura. The land is undulating and has many tiny rivulets. These rivulets are dry except during rains. In some part of this area, the Red soil is present. The soils are colored red or brown. This soil associated occupies almost a flat topography. Colluvial and Skeletal soil occur in the Bankura. These soils contain a large amount of coarse sand and gravel.

2.2. Data sources

In this study, three base years are defined to analyze LULC changes in Dwarakeswar Basin. Among all available satellite data, the following scenes were chosen: Landsat-5 Multispectral Scanner System (MSS) April 11, 1990 and December 23, 1990; Landsat-Thematic Mapper (TM) March 29, 2000 and November 8, 2000 and Landsat-7 Enhanced Thematic Mapper Plus (ETM+) April 2, 2010 and November 12, 2010. Both Pre-monsoon and Post Monsoon images of a particular year were used to assess the cropland areas of our study area. Landsat images are collected from Earth Explorer (http://earthexplorer.usgs.gov/) and Global Visualization (Glovis) (http://glovis.usgs.gov/). Because of the geographic location and the tropical climate, the area of Dwarakeswar watershed is frequently covered by cirrus and cumulus clouds. As a consequence, only a limited number of cloud-free optical satellite images are available for the study area. The data acquisitions used in this study cover different seasons (dry season to wet season) which has to be accounted for in the change detection analysis due to seasonal effects. GCM (HadCM3) data are used for climate change scenarios (URL:www.cccsn.ec.gc.ca). Temperature and precipitation data (station data) are collected from India Meteorological Department (IMD). Soil and geology maps collected from NBSS & LUP and Geological Survey of India. Groundwater level data are collected by the Central Ground Water Board.

2.3. Framework of the proposal

The methodology is divided into three sections (i) climate change modeling (ii) LULC change modeling and (iii) land suitability modeling. SDSM, Dyna-CLUE, AHP models are used for estimation of future scenarios. Three models are simulated from a small region to continent. It is flexible and generic modeling framework.

2.3.1. SDSM for future climate change predictions

The Global Climate Model (GCM) data have a coarse spatial resolution. Downscaling is required to extract the regional level information (Dorji et al., 2017). Observed and GCM data are needed for estimating of future climate change scenarios using Downscaling technique. SDSM considers five discrete processes (screening of predictor variables, model calibration, and synthesis of observed data, generation of climate change scenarios, and diagnostic testing and statistical analyses). At first, the SDSM input data file is predict and (atmospheric variables in meteorological stations). Then predictors (the screened large-scale climate variables from NCEP) are defined and screened. Predictand data sets used are daily maximum and minimum temperature and precipitation data. HadCM3 data (Kumar et al., 2006; Shukla et al., 2015)

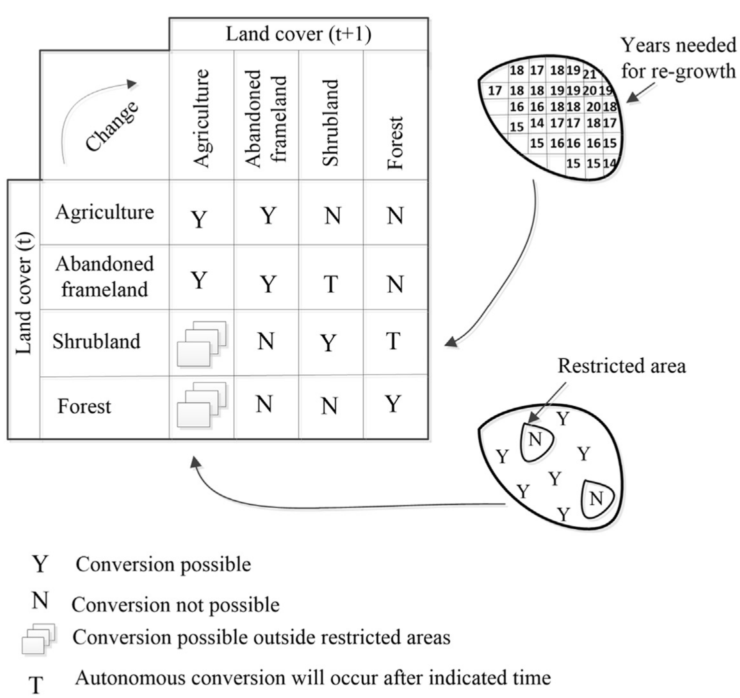

Fig. 2. Simplified land cover conversion matrix indicating the possible conversions.

are used for future climate change scenarios in the study area. HadCM3 data are collected from the National Centers for Environmental Prediction (NECP). SDSM included multivariate statistical analysis and weather classification system (Saymohammadi et al., 2017). Second, multi-linear regression analysis is used for calibration purpose. A Quality check function is used of the identify errors for calibration. Finally, the SDSM model is generating current and future estimation results.

2.3.2. Dyna-CLUE model for future LULC change predictions

Dynamic Conversion of Land-Use and its Effects (Dyna-CLUE) is a hybrid model for the dynamic simulation of competition between land-use types (Verburg et al., 2002). The Dyna - CLUE model is considered as a spatial allocation module and non-spatial demand module (Zhang et al., 2015). Spatial allocation module represents conversion between demands into land use changes at the different location in the study area (Fig. 2). The non-spatial module represents the area demands all land use features. The Dyna-CLUE model considers five types of input files (i.e., land-use demands, location suitability, neighborhood suitability, spatial restrictions and conversion parameters). LULC transformation is expected to take place at locations with the highest 'preference'. Preference indicates the interaction between the different features and decision-making system. The preference of a location is estimated from a set of features that are based on the different, disciplinary, understandings of the determinants of LULC change. The preference is calculated following:

$$R_{ki} = a_k X_{1i} + b_k X_{2i} + \ldots.. \quad (1)$$

where, R is the preference to devote location i to land use type k, $X_{1,2,\ldots}$ are biophysical or socio-economical characteristics of location i and a_k and b_k the relative impact of these characteristics on the preference for land use type k.

The stepwise logistic regression method is used for location suitability and neighborhood suitability for each land-use type.

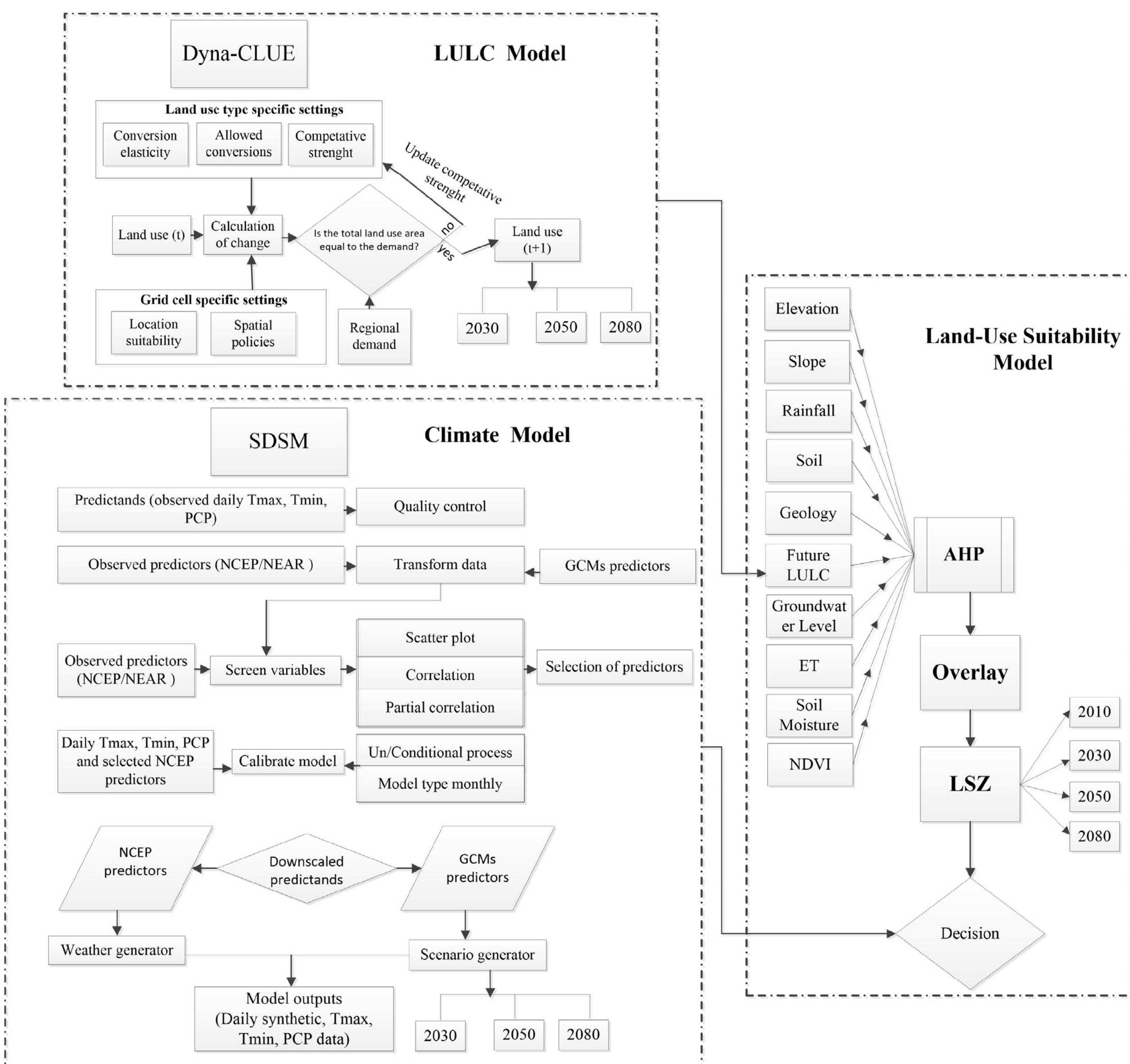

Fig. 3. Overall methodology.

Logistic regression can be calculated as (Verburg et al., 2002)

$$Log\left(\frac{P_i}{1-P_i}\right) = \beta_0 + \beta_1 X_{1,i} + \beta_2 X_{2,i........} + \beta_n X_{n,i} \quad (2)$$

Where, P_i is the probability of a grid cell for the occurrences of the considered land-use features. X's are the driving factors. Based on the logistic regression results: provides the coefficients with the driving forces, used to derive the Pi. Verburg et al. (2002) discuss the detailed stepwise procedure for the probability of a grid cell for the occurrences of the considered land-use features.

Aspect, elevation, slope, rainfall, temperature, soil depth, geology, distance from the road, distance from the rail, distance from the river, distance from built-up, distance from crop land, distance from forest cover are considered as driving factors. All spatial data are converted into a regular grid (250 m × 250 m). Finally, probability map can be created for each land–use features based on regression results. The model structure is composed the hierarchical organization of land-use systems, allowing for a continuous iteration between the local level and regional level demands.

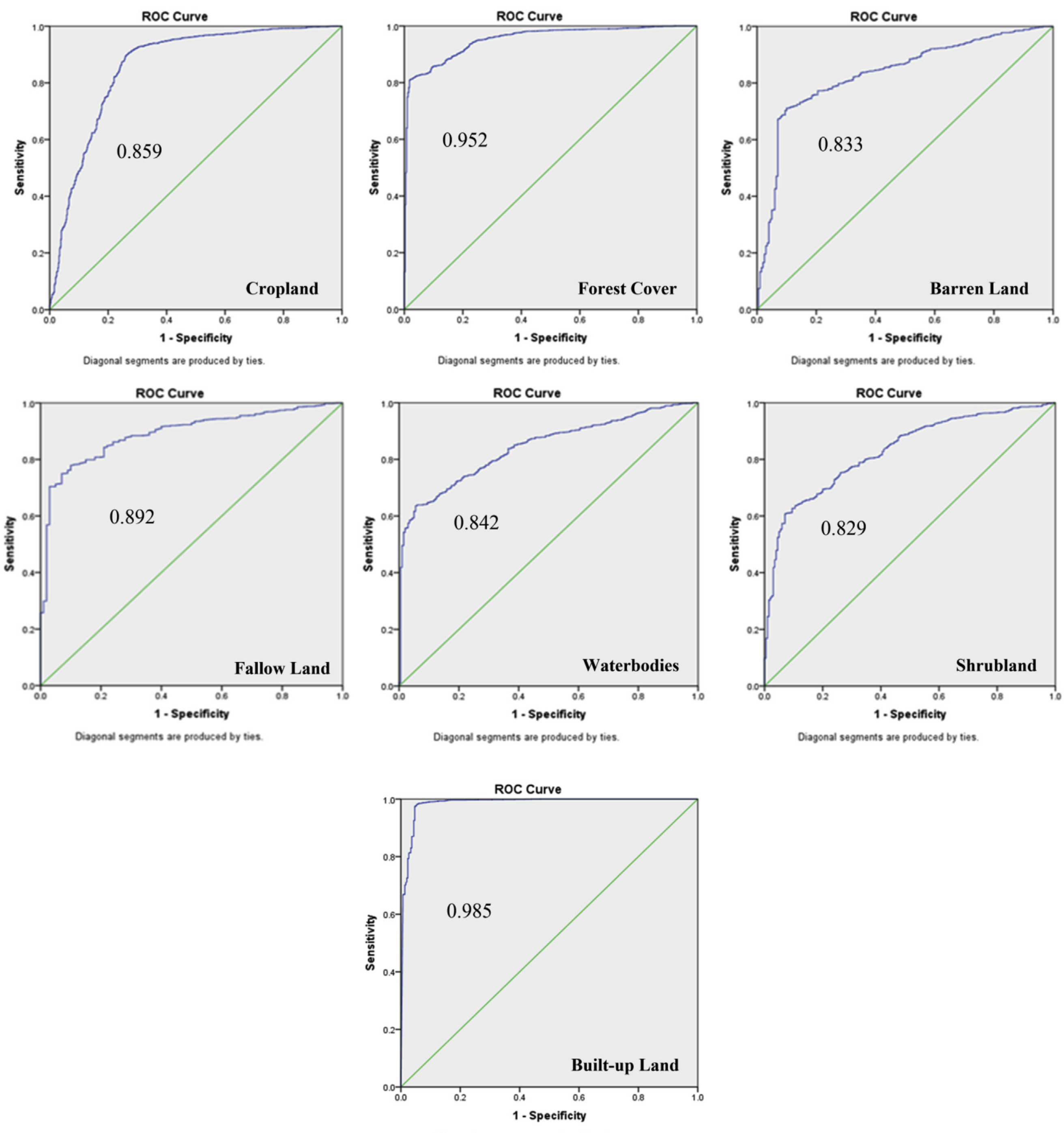

Fig. 4. ROC curve of all LULC features.

2.3.3. Land suitability zone mapping using analytic hierarchy process

The analyze of land use, suitability zone based on multi-criteria decision making (MCDA) system using GIS technique. Ten hydro-meteorological parameters (Elevation, slope, rainfall, soil, geology, future LULC, groundwater level, ET, NOAH based soil moisture and NDVI) are utilized for past and future LSZs in the river basin. Analytic hierarchy process (AHP) is the one of the best MCDA technique and the systematic approach (Alharthi et al., 2015; Ivanco et al., 2017). Comprehensive literature review and asking local expert opinions is help for weights assigned to various hydrogeological parameters. Then, AHP used to calculate weights often feature maps for LSZs. AHP^{LSI} can be calculated as (Sahoo et. 2016)

$$AHP^{LSI}|_{px,py} = \sum_{i=1}^{N_F} W_i C^{v}_{px,py}\Big|_i \tag{3}$$

Where, index i denotes feature; N_F is the total number of features; W_i the normalized weight of ith feature; $C^{v}_{px,py}\Big|_i$ denotes the class value of the cell (px, py) for ith feature. AHP can be applied for estimation of W_i. AHP provides a practical way to establish a relationship between the pairwise comparison matrixes. Saaty (1980) 1–9 scale is adopted for constructing judgment matrices. The following steps are adopted for the calculation of weights and the consistency ratio (C.R.):

Development of judgment matrices (**A**) by pairwise comparison.

Calculation of relative weight W_i:

$$W_i = GM_i \Big/ \sum_{m=1}^{N_F} GM_m \tag{4}$$

where the geometric mean of the ith row of judgment matrix is calculated as $GM_i = \sqrt[N_F]{a_{i1}a_{i2}\ldots a_{iN_F}}$.

Strength assessment of judgment matrix based consistency ratio (C.R.)

$$C.R. = C.I./R.C.I. \tag{5}$$

Consistency index (C.I.) is evaluated as

$$C.I. = \frac{\lambda_{\max} - N_F}{N_F - 1} \tag{6}$$

where, the latent root of judgment matrix is calculated as

$$\lambda_{\max} = \sum_{m=1}^{N_F} \frac{(\mathbf{AW})_m}{N_F W_m} \tag{7}$$

Where, **W** is the weight vector (column). Random consistency index (R.C.I.) can be obtained from standard tables. C.R. value less than 0.1 is acceptable for a specific judgment matrix. However, revision in judgment matrix is needed for C.R. $\geq$ 0.1. Finally, the LSZ zone map can be generated by using equation (3). Overall methodology is shown in Fig. 3.

2.3.4. Accuracy assessment of LULC

Accuracy assessment is performed for all the generated LULC maps. A total of 70 numbers of reference pixels (10 pixels per class) is selected for each generated LULC map. The reference pixels for the year 2000 and 2010 are verified from Google earth images. Future LULC (2030, 2050 and 2080) maps are also verified from the same google earth images. The overall accuracy and kappa statistics are used to assess the classification accuracy. The comparison between predicted results and reference data was presented statistically using error matrices. Error matrixes are generated based on the agreement between the classified image and the reference pixels. Overall accuracy is estimated by summing the number of pixels classified correctly divided by the total number of pixels. The kappa coefficient is estimated using the following equation:

$$K_c = \frac{(N \times \chi_{ii}) - (\chi_{i+} \times \chi_{+i})}{(N \times \chi_{i+}) - (\chi_{i+} \times \chi_{+i})} \tag{8}$$

Where, x_{ii} is the number of observations correctly classified in a particular category, x_{i+} and x_{+I} is the marginal totals for the row i and column i associated with the category and N is the total number of observations in the entire error matrix.

2.3.5. Sensitivity analysis

A leave-one-out approach is adopted for sensitivity analysis. Major changes due to the removal of a particular feature layer indicate the influence of that layer on the outcome. Influencing features can be identified by using sensitivity analysis as:

$$DS_i^j = S_{-i}^j - S_F^j \tag{9}$$

Where i is the subscript for a feature, $j$is the superscript for LSZs category. DS_i^j is the change (+/−) in LSZs area, S^j_{-i} is the jth type of LSZs area without ith feature, and S_F^j is the j th type of LSZs area using all feature.

Table 1
Calculated beta coefficients and ROC values of binary logistic regression for land use classes of 1990.

Driving Factors	CL	FC	BL	FL	WB	SL	BU
Road	−0.001	0.005	−0.001	0.000	0.002	−0.001	−0.001
Slope	−0.137	0.315	0.140	−0.027	0.096	0.291	−0.064
Soil	0.024	0.031	0.015	−0.119	0.022	0.209	−0.036
DBU	−0.001	0.015	0.018	0.009	0.002	0.016	−0.384
DCL	−0.013	0.003	0.012	0.015	0.003	0.011	−0.003
DFC	0.003	−0.022	0.011	0.017	0.003	0.018	20.953
Aspect	0.004	−0.002	−0.001	0.004	0.001	−0.001	−0.002
Elevation	−0.002	0.019	−0.008	0.008	−0.027	0.011	−0.011
Geology	0.167	0.126	0.301	0.014	0.600	−0.067	−0.219
Rail	−0.002	0.001	0.014	0.003	0.005	−0.004	−0.007
Rainfall	−0.281	2.062	−0.168	0.934	−0.737	0.491	−0.170
River	0.000	3.644	0.007	0.582	−0.021	0.007	−0.003
β Constant	29.481	1130.078	4.163	−246.346	73.814	−56.277	−633.877
ROC values	0.859	0.952	0.833	0.892	0.842	0.829	0.985

3. Results and discussion

3.1. Analysis of drivers concerning LULC classes

The results of the Dyna-CLUE model provide scenarios of future LULC within the study area following three differing years for the period 2030, 2050, 2080 which are differentiated by the demands of LULC types. These LULC types are further analyzed using the different driving factors (Fig. 4). From the binary logistic regression analysis (Table 1) of the cropland class for the year 1990, the driving factors like soil, aspect, geology, distance to forest cover, distance to river showed positive values indicating more probability of occurrence of the cropland class with a ROC curve of 0.859 implying the acceptability of the regression analysis. In the case of forest cover soil, geology, distance to road, distance to river, slope, elevation, distance to built-up, rainfall, distance to rail affect more occurrence of forest cover generating an overall accuracy of 0.952 in the area under the ROC curve. After analyzing the class, barren land it was found that the factors like soil, geology, distance to cropland, distance to forest cover, distance to river, Slope, distance to built-up, distance to rail affect more occurrence of barren land and it showed an overall accuracy of 0.833 implying the acceptability of the regression analysis. Fallow land showed similar results like forest cover with a ROC curve of 0.892 followed by water bodies with an overall accuracy of 0.842. From the regression results of built-up land, it could be interpreted that more probability of occurrence of the built-up class is due to driving factors like distance to road, aspect, distance to rail, geology, distance to cropland, distance to forest cover, distance to built-up, distance to rail. The ROC curve of built up was the highest giving an overall accuracy of 0.985 implying the acceptability of the regression analysis.

3.2. Analysis of future climate change predictions

Climate change predictions have been performed for the three scenarios (2030, 2050 and 2080) in the river basin (Sahoo et al. 2018). SDSM is utilized for downscaling of general circulation model to station scales. Two scenarios (A2 and B2) are available

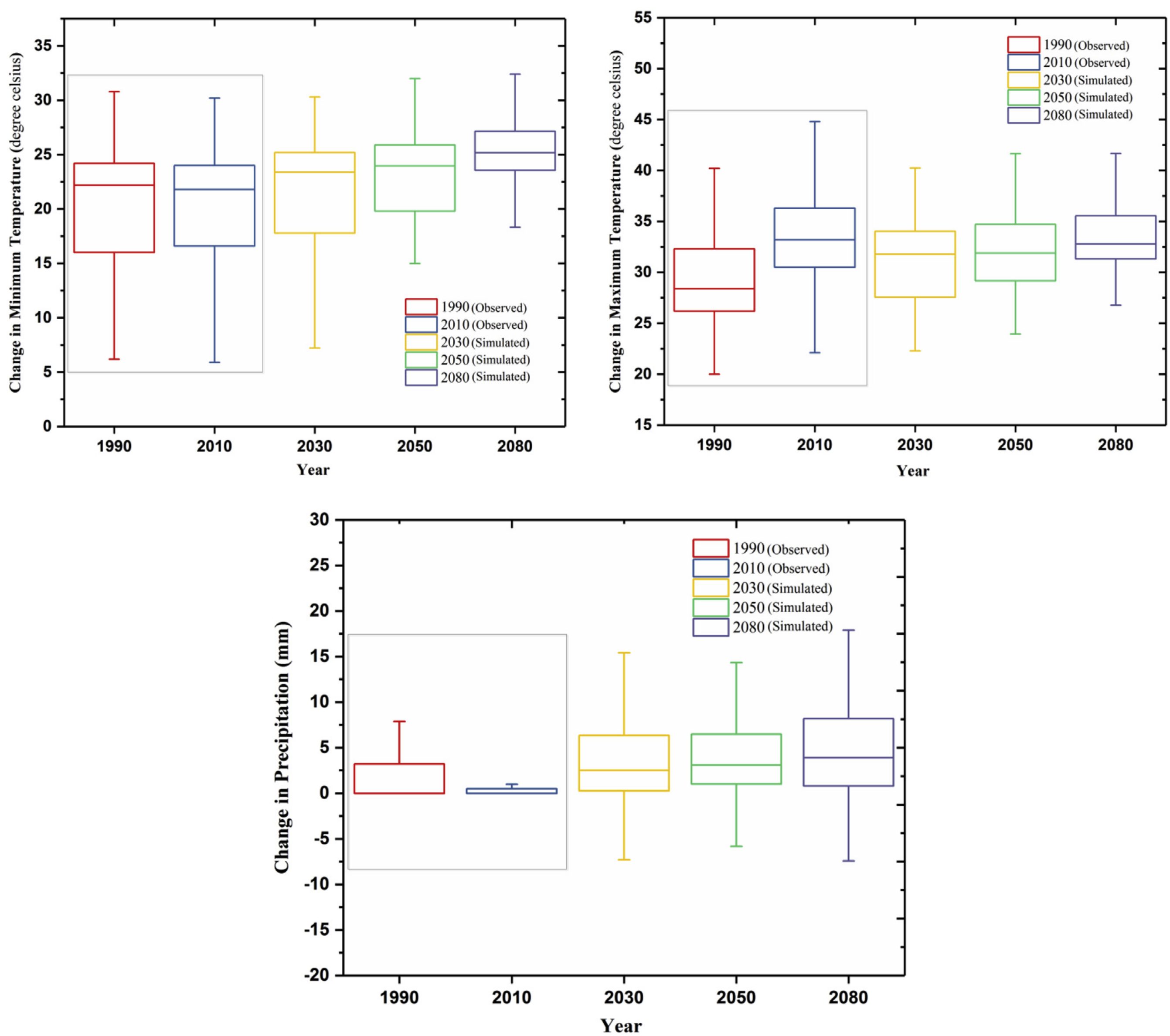

Fig. 5. Graphical representation of simulated and observed temperature and precipitation.

under HadCM3 [from a spatial resolution of 2.5° (latitude) by 3.75° (longitude)]. A2 scenario (continuously increased population and regionally oriented economic development based data) is considered for calibration and validation. B2 is not utilized as it considers continuously increased population, but a slower rate than A2 and intermediate levels of economic development. The daily temperature and rainfall data are utilized for calibration from 1990 to 2010 and validated from 2011 to 2016. Predicted temperature and precipitation graphs are shown in Fig. 5. Simulated temperature and precipitation results show increasing and decreasing trends, respectively.

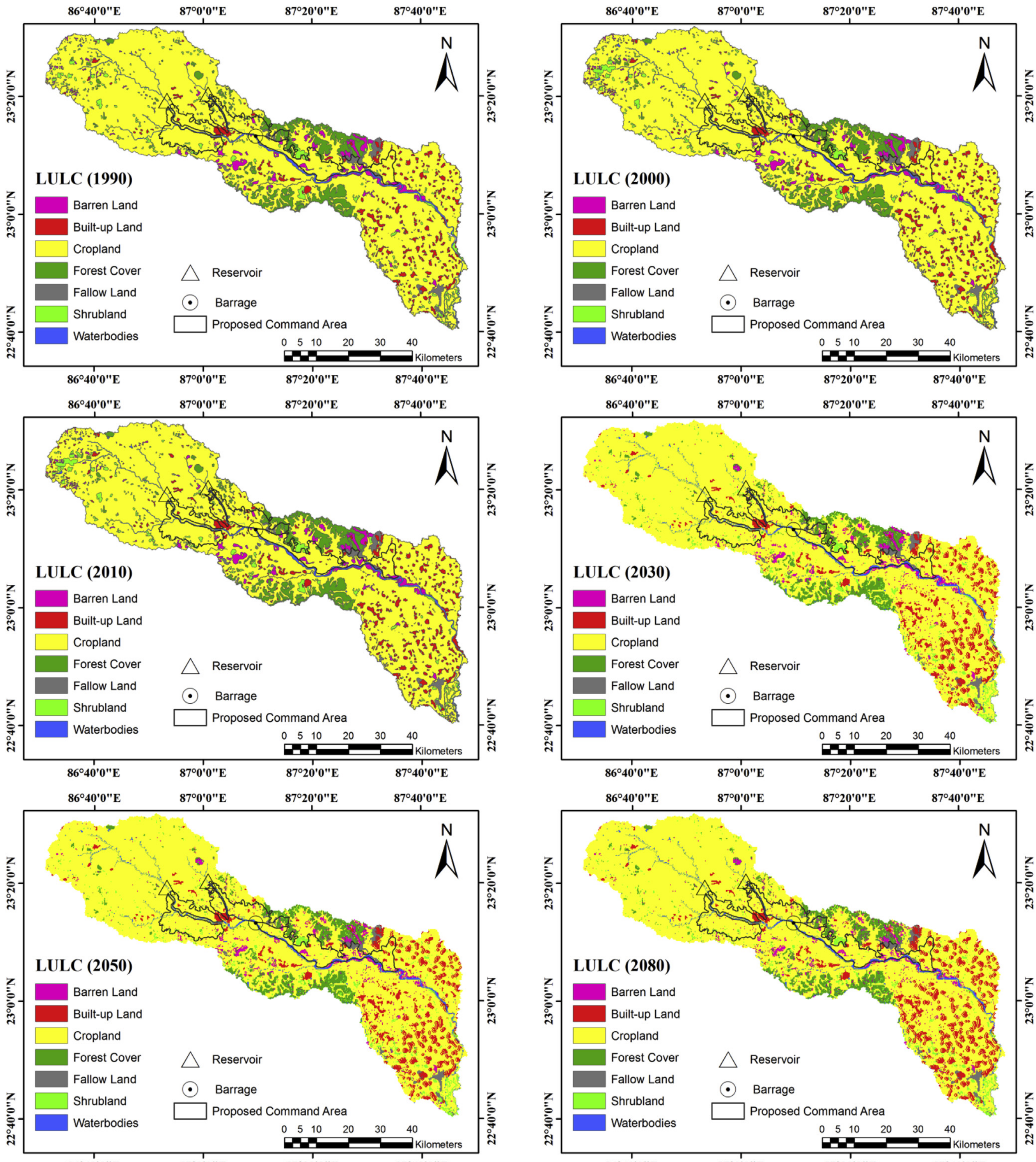

Fig. 6. Observed and simulated LULC Mapping.

3.3. Analysis of LULC change

LULC maps for the year 1990, 2000 and 2010 are prepared using remote sensing technique in the river basin (Fig. 6). The analysis also focuses on LULC mapping in the proposed command area (Fig. 7). Numerous polygons are manually digitized with the help of visual interpretation of the Landsat image based on the author's knowledge of the study area and converted to raster for further analysis. Classified maps are compared to detect the change in LULC. The generated LULC maps showed cropland (CL), forest

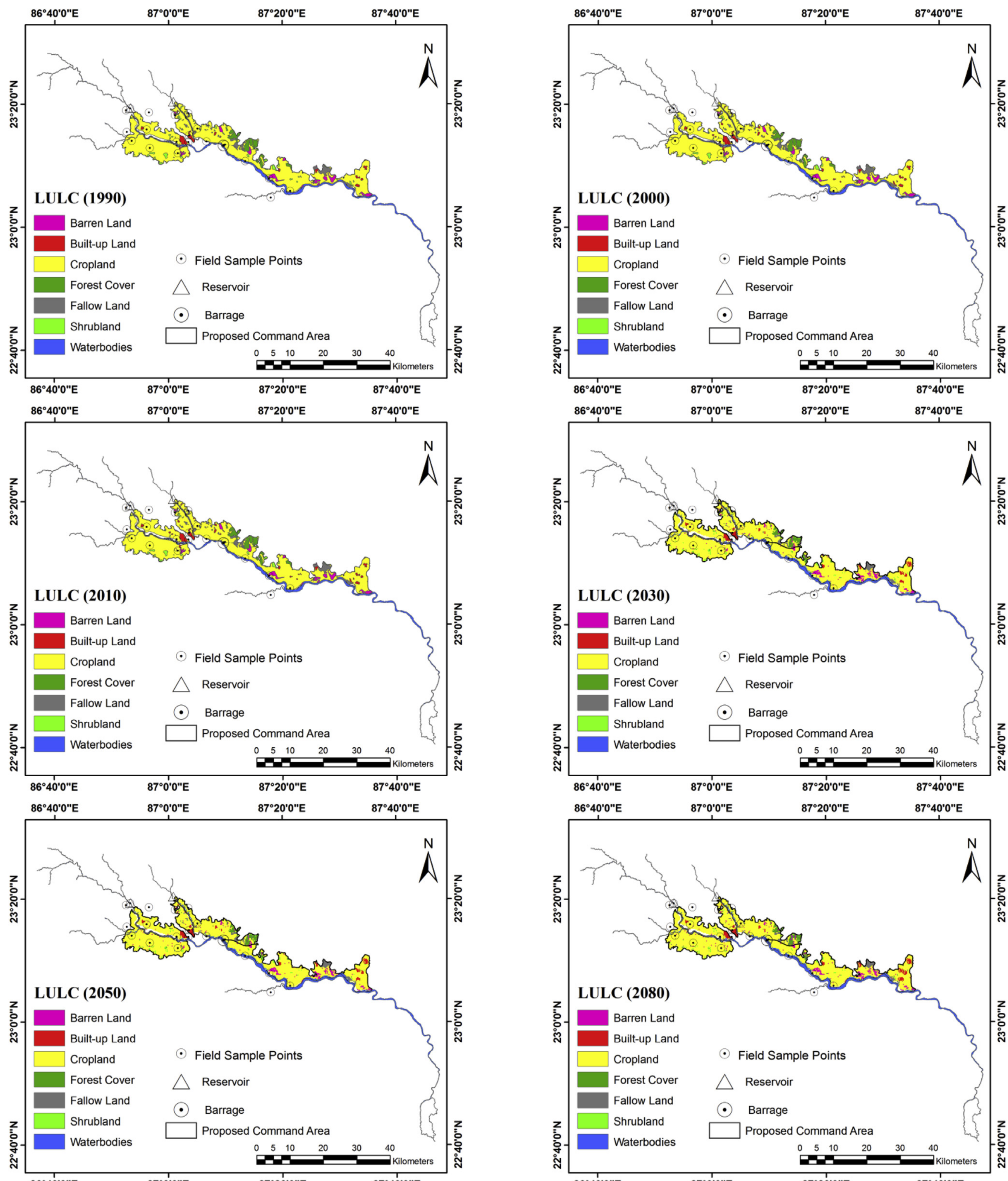

Fig. 7. Observed and simulated LULC mapping of proposed command area.

Table 2
Area of different LULC classes during different years in the Dwarakeswar - Gandheswari river basin.

LULC class	1990 (Ha)	2000 (Ha)	Change (Ha)	2010 (Ha)	2030 (Ha)	Change (Ha)	2050 (Ha)	2080 (Ha)	Change (Ha)
CL	346620.30	344564.00	−2056.30	344056.50	343251.50	−805.00	342432.70	340363.90	−2068.80
FC	28043.75	27781.25	−262.50	27325.00	26325.00	−1000.00	25581.30	24475.00	−1106.30
BL	12262.50	12650.00	+387.50	12487.50	12337.50	−150.00	11912.50	11556.30	−356.20
FL	6700.00	6687.50	−12.50	6787.50	6837.50	+50.00	7143.75	7431.25	+287.50
WB	7506.25	7662.50	+156.25	7682.50	7506.25	−176.25	7506.25	7506.15	−0.10
SL	13187.50	12425.00	−762.50	12225.00	11862.50	−362.50	11587.50	10981.30	−606.20
BU	19856.25	22406.25	+2550.00	23612.50	26056.30	+2443.80	28012.50	31862.50	+3850.00

Table 3
Percentage of area of different LULC classes during different years in the proposed command area.

LULC class	1990 (%)	2000 (%)	Change (%)	2010 (%)	2030 (%)	Change (%)	2050 (%)	2080 (%)	Change (%)
CL	82.06	82.90	+0.846	82.93	82.31	−0.620	82.41	82.43	+0.02
FC	4.37	4.42	+0.051	4.42	3.46	−0.961	3.28	2.99	−0.29
BL	4.26	3.75	−0.509	3.71	3.65	−0.060	3.66	3.62	−0.03
FL	3.23	3.27	+0.038	3.27	2.59	−0.686	2.66	2.42	−0.23
WB	1.15	1.16	+0.014	1.16	3.87	+2.705	3.87	3.87	+0.00
SL	2.34	1.75	−0.590	1.67	1.38	−0.291	1.30	1.22	−0.08
BU	2.60	2.75	+0.149	2.83	3.27	+0.440	3.36	3.44	+0.08

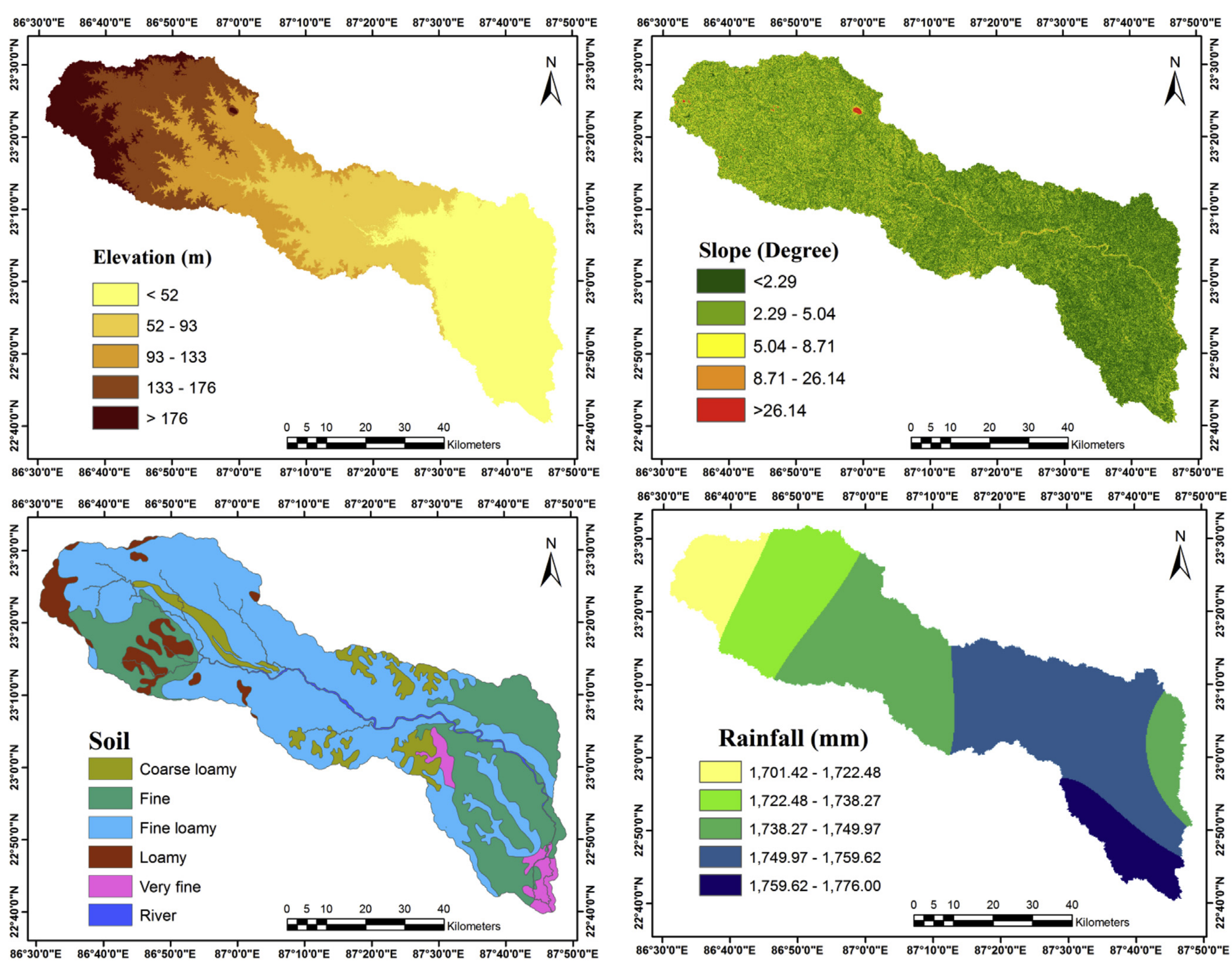

Fig. 8. Elevation, slope, soil and rainfall.

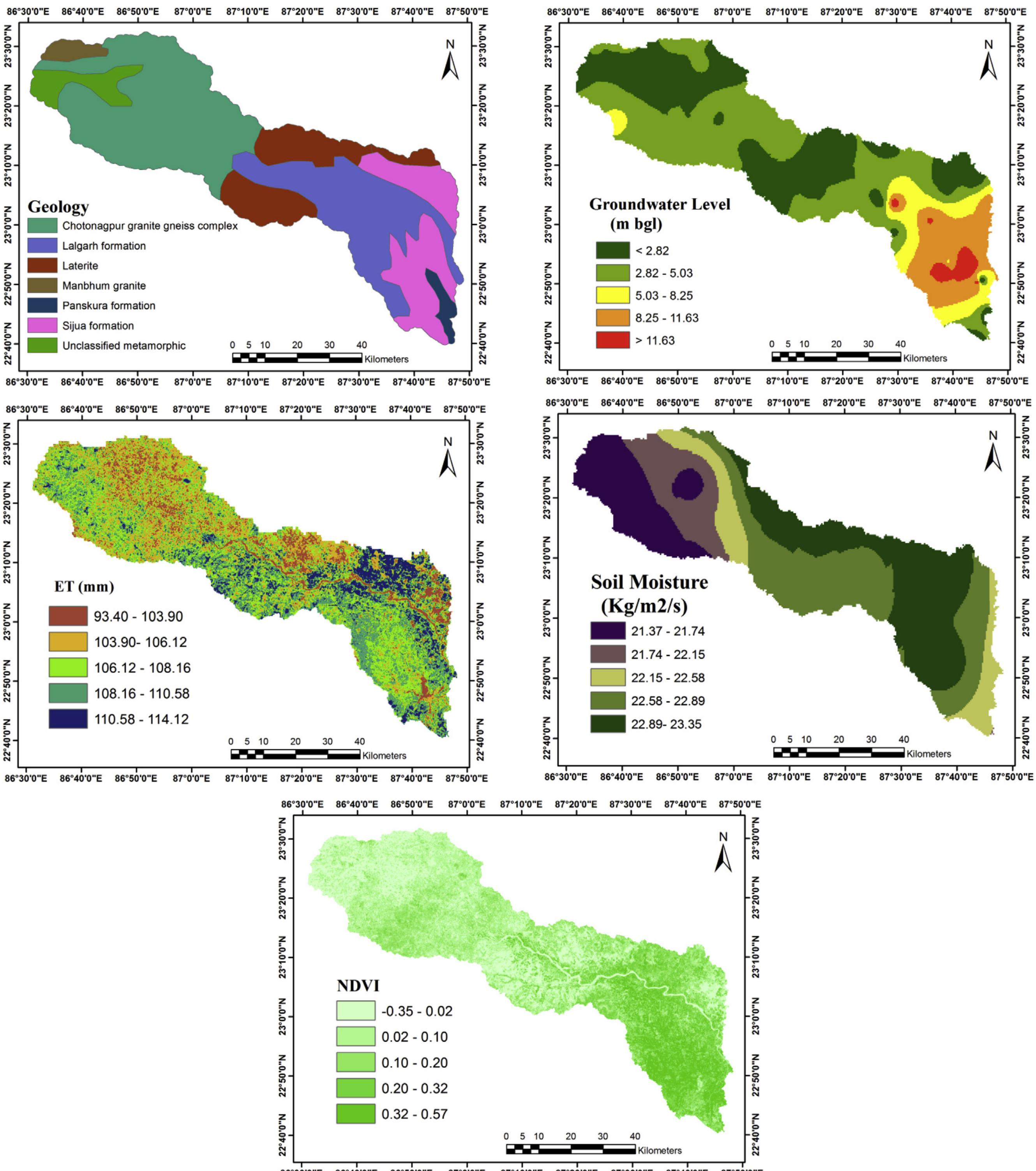

Fig. 9. Geology, groundwater level, ET, soil moisture and NDVI map.

covers (FC), barren land (BL), fallow land (FL), water bodies (WB), shrubland (SL), and built-up land (BU) classes, their distribution, and spatial extent. The result shows that cropland, forest cover, and shrubland are decreased in 1990, 2000 and 2010 respectively (Table 2). The size of the cropland decreased by 0.47% between 1990 and 2000. Between the 2000 and 2010, the size of built-up land increased by 0.28%. The results also show that barren land, fallow land, and water bodies are increased and decreased in 1990, 2000 and 2010. The only built-up land is increased continuously. Error matrices are very important to how many references pixels are correctly classified. The columns represent which classes the pixels are in the reference pixels. The rows represent which classes the image pixels have been assigned to in the image. The diagonal represents pixels are classified or predicted correctly. Error

Table 4
Pair-wise comparison matrix (ten attribute layers) developed for AHP based land suitability index.

Features	Elevation	Slope	Rainfall	Soil	Geology	Future LULC	Groundwater Level	ET	Soil Moisture	NDVI	Normalized Weights
Elevation	8/8	8/4	8/5	8/3	8/2	8/6	8/3	8/4	8/7	8/1	0.1860
Slope	4/8	4/4	4/5	4/3	4/2	4/6	4/3	4/4	4/7	4/1	0.0930
Rainfall	5/8	5/4	5/5	5/3	5/2	5/6	5/3	5/4	5/7	5/1	0.1163
Soil	3/8	3/4	3/5	3/3	3/2	3/6	3/3	3/4	3/7	3/1	0.0698
Geology	2/8	2/4	2/5	2/3	2/2	2/6	2/3	2/4	2/7	2/1	0.0465
Future LULC	6/8	6/4	6/5	6/3	6/2	6/6	6/3	6/4	6/7	6/1	0.1395
Groundwater Level	3/8	3/4	3/5	3/3	3/2	3/6	3/3	3/4	3/7	3/1	0.0698
ET	4/8	4/4	4/5	4/3	4/2	4/6	4/3	4/4	4/7	4/1	0.0930
Soil Moisture	7/8	7/4	7/5	7/3	7/2	7/6	7/3	7/4	7/7	7/1	0.1628
NDVI	1/8	1/4	1/5	1/3	1/2	1/6	1/3	1/4	1/7	1/1	0.0233

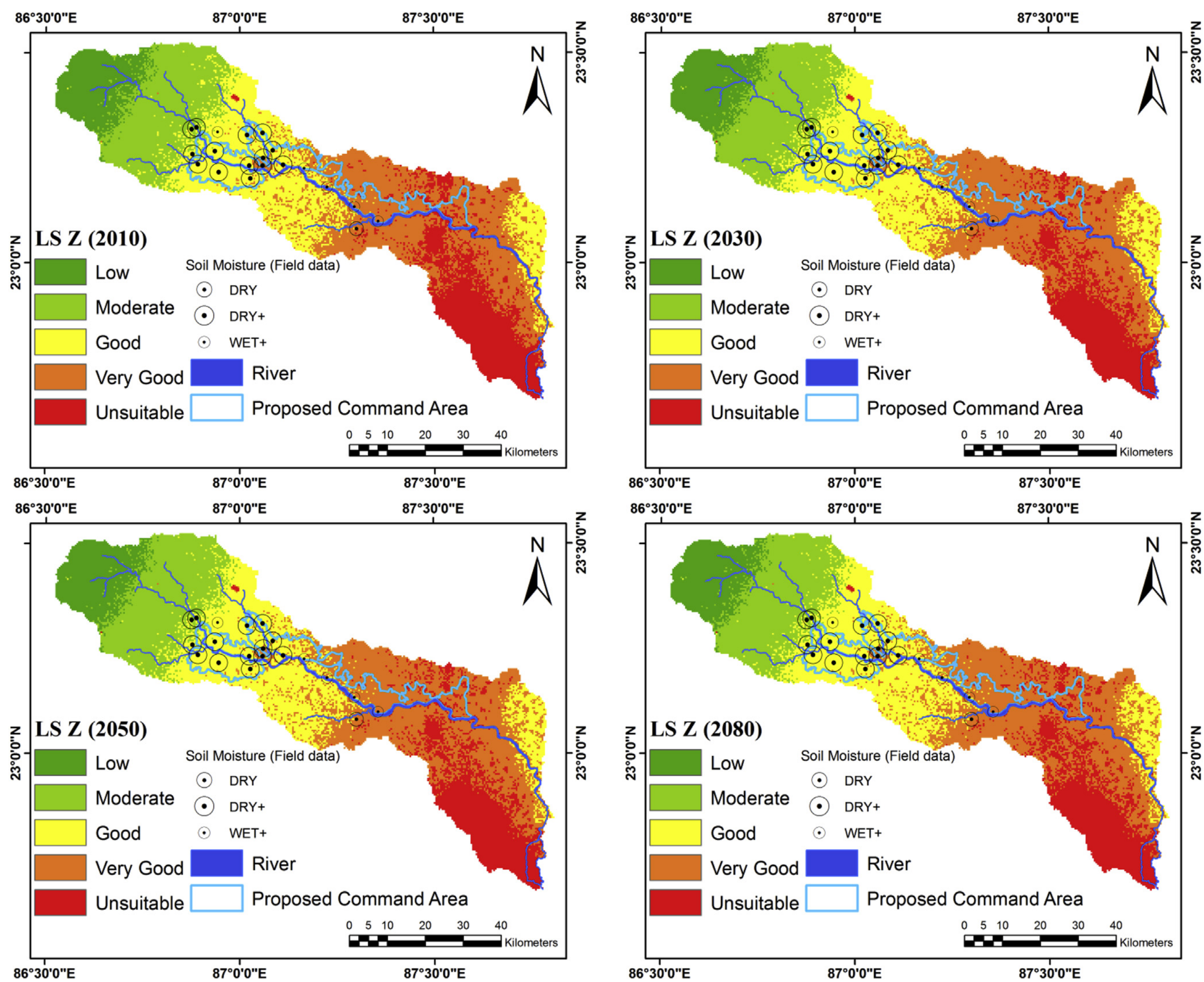

Fig. 10. Future scenarios of land suitability zones mapping for agriculture sustainability.

matrices (SM 1- SM 3) are generated for classification accuracy assessment of the LULC maps for the year 1990, 2000, and 2010. For all the years 1990, 2000 and 2010 accuracy assessments show the overall accuracy of 94.29, 95.79, 95.00 and overall Kappa coefficient of 0.94,0.95 and 0.95 respectively. Change matrix SM 4, and SM 5 is a result of the LULC change detection analysis between 1990, 2000 and 2010.

3.4. Analysis of future LULC change predictions

LULC maps developed in the years 1990, 2000 and 2010 along with the future predicted LULC maps for the year 2030, 2050 and 2080 (Fig. 6). The simulated result shows that there is a total of 344056.50 ha of cropland in 2010 and in 2030 it decreased by 825 resulting in 343251.50 ha. It can be observed from Table 2 that most of the cropland has been converted to built-up land. The results also

show that fallow land and built-up land area increased by 0.07% and 0.89% between 2050 and 2080. Change detection matrixes are generated for future LULC classes (SM 6- SM 8). It can be seen that 2010–2030 show a significant change in the LULC classes. After 2030–2080 shows that there is no significant change in the LULC classes of the river basin. The future prediction of LULC results also focuses on the proposed command area (Table 3). Proposed command area maximum covered by the cropland feature.

3.5. Analysis of future land suitability zones predictions

Elevation, slope, rainfall, soil, geology, future LULC, groundwater level, ET, soil moisture and NDVI have considered for the land suitability index (LSI) calculation (Figs. 8 and 9). Elevation map is generated from SRTM DEM (grid: 30 × 30). Slope calculated from elevation data. Soil moisture is very important for crop water stress distribution. A soil moisture map prepared from NOAH land surface model L4 monthly 0.25° × 0.25° V001 (URL:https://disc.sci.gsfc.nasa.gov). ET is important to know how much water is required during the growing season, to improve crop water management. Estimation the ET map based on the FAO Penman-Monteith method using the Landsat 8 OLI satellite data (Zotarelli et al., 2010). The lower part of the river basin is showing the higher ET values, and also in the Jangalmagal area and some portion of the Purulia district ET value is high. Moreover, it could be said, ET variations in this study are closely related to crop growth. When paddy fields are empty, and the fields are covered by very small vegetation, ET values are low. But in cropping season and in the monsoon, when vegetation cover is dense, ET values are high. All parameters prepared from GIS platform. The groundwater level is a comprehensive expression of LSZ. Groundwater level value varies <2.82 bgl m - >11.63 bgl m. One scenario for 2010 and three future scenarios for 2030, 2050 and 2080 are generated based on AHP weights (Table 4) using the weighted overlay method. Future scenarios of LSZs are simulated based on future LULC and recent parameter maps. The resultant LSI map for agricultural sustainability is classified into five zones (Fig. 10) (i) poor, (ii) moderate (iii) good (iv) very good and (iv) unsuitable. The results show that unsuitable zone is visible for all years in the downstream of the river basin because of a highly built-up area. The results also show that the middle portion of the river basin cover of the good and very good land-use suitability zones. The upstream of the river basin shows that moderate and poor suitability zone because of the high water stress zone. So, two reservoirs and one barrage will be constructed on Dwarakeswar and Gandheswari rivers for sustainable integrated water management. Areas of different classes change detection analysis between 2010 -2030 and 2050–2080 shown in Table 5. Moreover, agricultural suitability increased far away areas with high water demand.

3.6. Sensitivity analysis of land suitability zones

Sensitivity analysis (SA) is very important for land suitability zone mapping. SA is permitted to evaluate ranking variability for the land suitability index (Sabia et al., 2016). SA also considered an area under the different class changes with exclusion of each parameter. Positive and negative values indicate the positive and negative weight changes for similar sensitivity (Qiu et al., 2017). The elevation is not significant for LSZ mapping. Slope, soil, geology, ET, and NDVI are moderately significant. It is observed that rainfall, groundwater level, LULC and soil moisture are the influencing features. Positive and negative higher value (e.g., Rainfall: +24.15) represent the very good and poor impact for PSZ. Sensitivity analyses are presented in Table 6.

4. discussions

Future prediction of LULC with climate change has been performed in the small river basin in West Bengal. The fewest number of researcher attempt this kind of analysis for irrigation management point of view. The complexities of the LULC system depend on climate change scenarios. The on-screen visual interpretation techniques (Roy et al., 2015) are used for LULC classification (e.g., 1990, 2000 and 2010). Visual interpretation shows that more quality controls over digital classification for analyzing medium resolution satellite data. Various hydro-meteorological and

Table 5
Area under different classes change for land suitability zones.

LSZs	2010 (%)	2030 (%)	Change (%)	2050 (%)	2080 (%)	Change (%)
Poor	8.66	8.59	−0.07	8.59	8.58	−0.01
Moderate	17.68	17.75	+0.07	17.74	17.73	−0.01
Good	25.44	26.30	+0.86	26.26	26.16	−0.1
Very Good	31.26	32.43	+1.17	32.39	32.08	−0.31
Unsuitable	16.96	14.94	−2.02	15.02	15.44	+0.42

Table 6
Area under different classes change with exclusion of each parameter.

% Change						
i		Poor	Moderate	Good	Very Good	Unsuitable
1	Elevation	0.00	0.00	0.00	0.00	0.00
2	Slope	−0.68	−1.35	+0.73	0.00	+1.30
3	Rainfall	**−20.40**	**−21.33**	**+2.55**	**+24.15**	**+15.03**
4	Soil	−0.61	−0.65	+1.72	−0.73	+0.26
5	Geology	−0.50	−0.50	+2.63	−0.42	−1.21
6	Future LULC	+1.14	**+3.30**	**+11.13**	−1.15	**−14.42**
7	Groundwater Level	+0.07	+0.19	**+2.77**	**−2.53**	−0.51
8	ET	−0.49	−0.59	+0.97	−0.10	+0.21
9	Soil Moisture	−0.17	−0.42	**−2.68**	−1.84	+5.11
10	NDVI	−0.49	−0.58	+0.96	−0.15	+0.26
S_F	All parameters	8.66	17.68	25.44	31.26	16.96

Bold values indicate significant results.

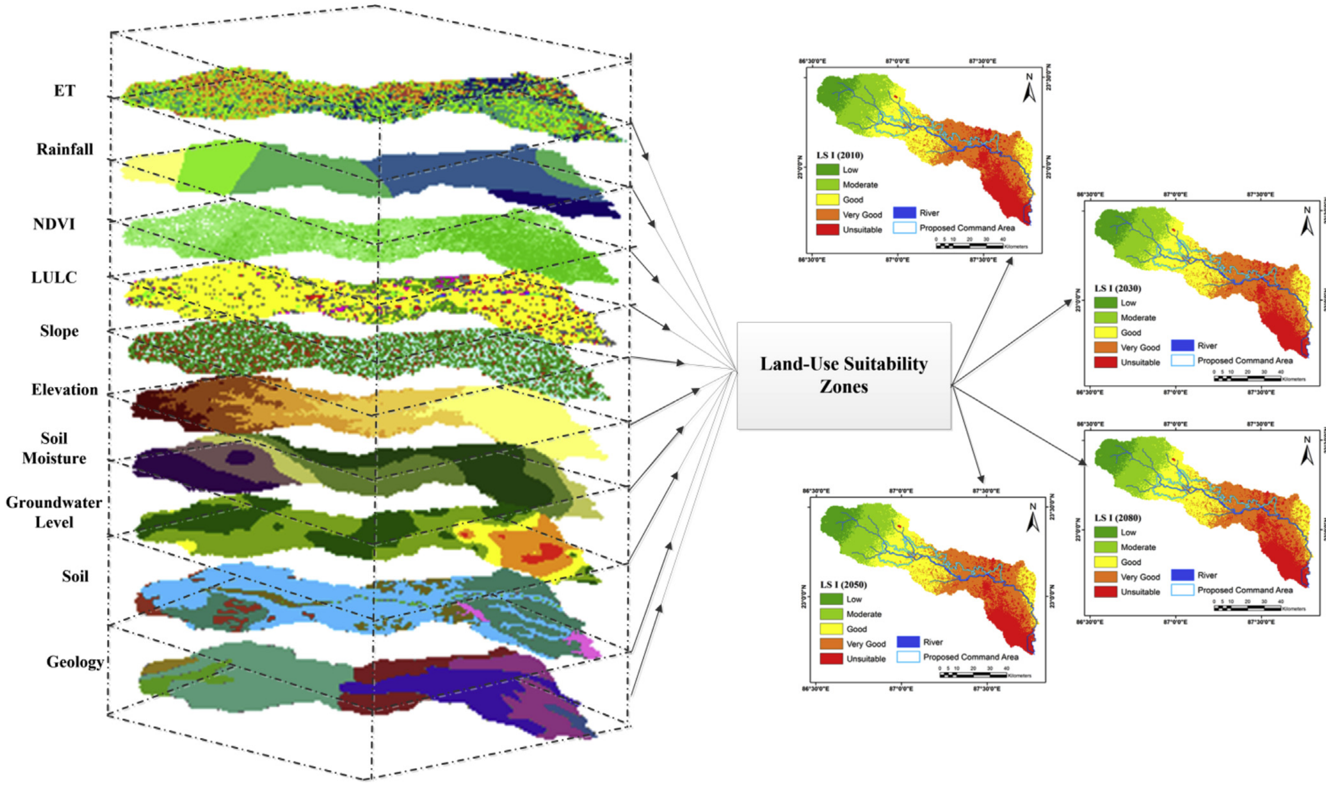

Fig. 11. Graphical representation of land suitability zone mapping.

geological parameters are used for significant impact on LULC change (Behera et al., 2017). Butt et al. (2015) studied the land use change mapping and analysis using remote sensing and GIS in the Simly watershed, Islamabad, Pakistan. Petz et al. (2016) created methodological documentation on indicators and modeling of land use, land management, and ecosystem services. CLUE model predicts the how the correct net quantity for each LULC type and location changes of LULC transition (Pontius et al., 2008). The future LULC change models help for future ecosystem balance response to changes. A Receiver Operating Characteristic Curve (ROC) is a standard technique for summarizing classifier performance (Swets, 1988). ROC curve is used for the parameters justification, the

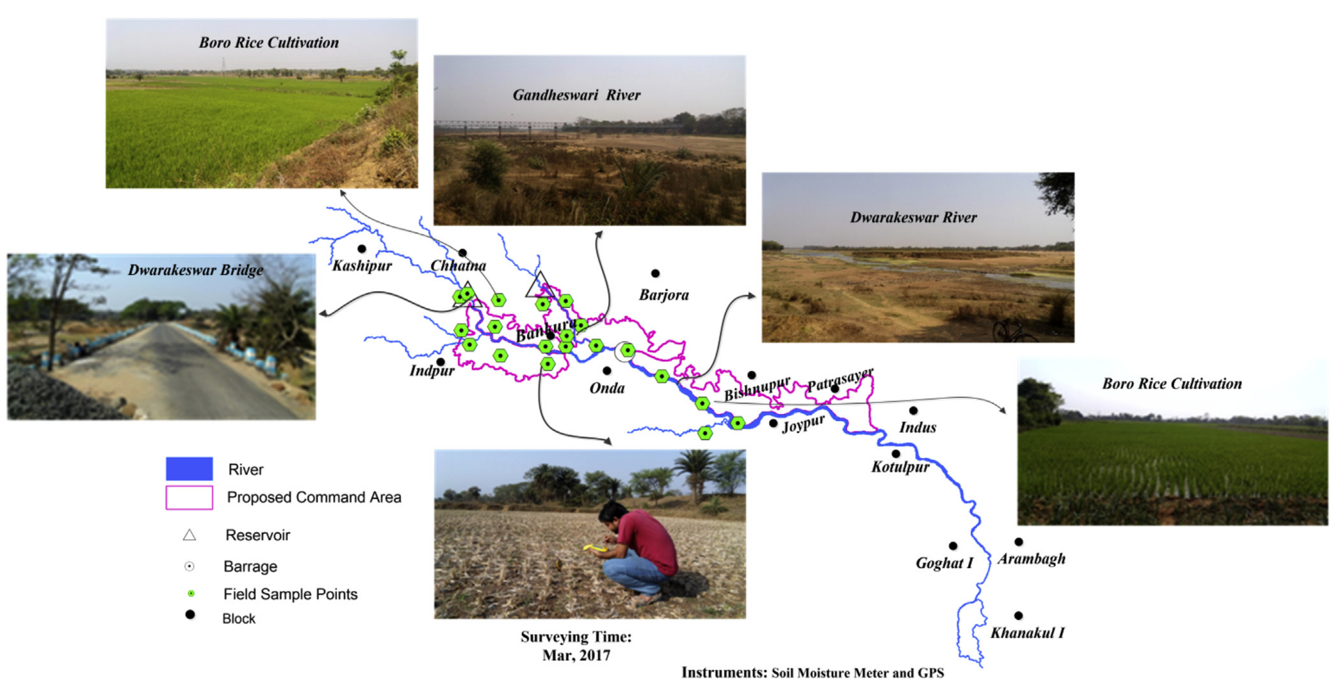

Fig. 12. Field survey, pictures of the proposed command area.

purpose of LULC model. Climate change is very important for in major socio-ecological transformations (Lopez et al., 2016). An LSZ model is constructed based on the AHP method using GIS environment. Agricultural LSZ mapping follow by the Geo-environmental features to local environmental condition for land evaluation (Elsheikh et al., 2013). Site selection of industrial wastewater discharge using Multi-criteria evaluation method in coastal regions is available in Li et al. (2017a, b). A close look of LSZ with the catchments indicates very high variation between different catchments (Yalew et al., 2016). This research work would be more accurate if more factors are taken into consideration. The simulation of future LSZ is important for the future land development pattern when the current land development process continues into the future (Li and Yeh, 2002). Graphical representation of LSZs is shown in Fig. 11. Field survey photographs of the proposed command area are shown in Fig. 12.

5. Conclusions

In this study, we present a framework for identification of future LSZs using the AHP method in the Dwarakeswar - Gandheswari river basin. A dynamic simulation model is used for future LULC change scenarios; then output maps are utilized for future land suitability zone mapping. LULC and climate change analysis are shown with three scenarios for the years 2030, 2050 and 2080. This research work mainly focuses on LSZs for agricultural sustainability. The cropland is the most dominant class for all the years, followed by forest cover, shrubland, and Built-up. The built-up land is 2030 showed 0.56% of growth rate while cropland has a degradation rate of 0.18%. During all the LULC scenarios highest change is noticed in the built-up class, which may be possible due to rapid population growth, urbanization, and industrial development. Four land-use suitability and one unsuitable zone are visible for the four scenarios in the river basin. The results also demonstrated that most of the area under suitability classes. The unsuitable zone is shown downstream of the river basin. Limitation of the CLUE model has been determined human behavior that leads to change LULC. This model is not straightforward and sensitive to the implementation of an initial LULC age of pixel. AHP model is an invariable weight system. So, the modified AHP model give us better results than AHP. Moreover, integrated spatial analysis, combining of decision criteria by modeling, sensitivity analyses and generation of maps are needed for land evaluation framework.

Acknowledgment

The authors thank Irrigation and Waterways Directorate, Government of West Bengal, India for providing necessary support for this research work. The authors also thank the India Meteorological Department for providing weather data for this research work.

Appendix A. Supplementary data

Supplementary data to this article can be found online at https://doi.org/10.1016/j.jclepro.2018.09.099.

References

Alharthi, H., Sultana, N., Al-amoudi, A., Basudan, A., 2015. An analytic hierarchy process–based method to rank the critical success factors of implementing a pharmacy barcode system. Perspect. Health Inf. Manag. 12 (Winter).
Amici, V., Marcantonio, M., La Porta, N., Rocchini, D., 2017. A multi-temporal approach in MaxEnt modelling: a new frontier for land use/land cover change detection. Ecol. Inf. 40, 40–49.
Aquilué, N., De Cáceres, M., Fortin, M.J., Fall, A., Brotons, L., 2017. A spatial allocation procedure to model land-use/land-cover changes: accounting for occurrence and spread processes. Ecol. Model. 344, 73–86.
Behera, M.D., Tripathi, P., Das, P., Srivastava, S.K., Roy, P.S., Joshi, C., Behera, P.R., Deka, J., Kumar, P., Khan, M.L., Tripathi, O.P., Dash, T., Krishnamurthy, Y.V.N., 2017. J. Eviron. Manag. 1–12.
Butt, A., Shabbir, R., Ahmad, S.S., Aziz, N., 2015. Land use change mapping and analysis using Remote Sensing and GIS: a case study of Simly watershed, Islamabad, Pakistan. Egypt. J. Rem. Sens. Space Sci. 18 (2), 251–259.
Choudhari, D.K., 2013. Uncertainty Modeling for Asynchronous Time Series Data with Incorporation of Spatial Variation for Land Use or Land Cover Change. University of Twente Faculty of Geo-Information and Earth Observation (ITC).
Dorji, S., Herath, S., Mishra, B.K., 2017. Future climate of colombo downscaled with SDSM-neural network. Climate 5 (1), 24.
EIA-EMP-Report, 2007. Irrigation and Waterways Directorate. Government of West Bengal, India.
Elsheikh, R., Shariff, A.R.B.M., Amiri, F., Ahmad, N.B., Balasundram, S.K., Soom, M.A.M., 2013. Agriculture Land Suitability Evaluator (ALSE): a decision and planning support tool for tropical and subtropical crops. Comput. Electron. Agric. 93, 98–110.
Han, H., Yang, C., Song, J., 2015. Scenario simulation and the prediction of land use and land cover change in Beijing, China. Sustainability 7 (4), 4260–4279.
Hoeppe, P., 2016. Trends in weather related disasters–Consequences for insurers and society. Weather Clim. Extremes 11, 70–79.
Igbokwe, J.I., Ezeomedo, I.C., Ejikeme, J., 2013. Identification of urban sprawl using remote sensing and GIS technique: a case study of Onitsha and its environs in Southeast, Nigeria. Int. J. Rem. Sens. Geosci. 2, 41–49.
Ivanco, M., Hou, G., Michaeli, J., 2017. Sensitivity analysis method to address user disparities in the analytic hierarchy process. Expert Syst. Appl. 90, 111–126.
Kumar, K.R., Sahai, A.K., Kumar, K.K., Patwardhan, S.K., Mishra, P.K., Revadekar, J.V., et al., 2006. High-resolution climate change scenarios for India for the 21st century. Curr. Sci. 334–345.
Le Roux, A., 2012. Quantifying the Spatial Implications of Future Land Use Policies in South Africa: Reshaping a City through Land Use Modelling. Doctoral dissertation. University of Utrecht, The Netherlands.
Li, X., Yeh, A.G.O., 2002. Neural-network-based cellular automata for simulating multiple land use changes using GIS. Int. J. Geogr. Inf. Sci. 16 (4), 323–343.
Li, Z., Wu, W., Liu, X., Fath, B.D., Sun, H., Liu, X., et al., 2017a. Land use/cover change and regional climate change in an arid grassland ecosystem of Inner Mongolia, China. Ecol. Model. 353, 86–94.
Li, Y., Lin, C., Wang, Y., Gao, X., Xie, T., Hai, R., et al., 2017b. Multi-criteria evaluation method for site selection of industrial wastewater discharge in coastal regions. J. Clean. Prod. 161, 1143–1152.
Liu, R., Zhang, K., Zhang, Z., Borthwick, A.G., 2014. Land-use suitability analysis for urban development in Beijing. J. Environ. Manag. 145, 170–179.
López, S., Wright, C., Costanza, P., 2016. Environmental Change in the Equatorial Andes: Linking Climate, Land Use, and Land Cover Transformations. Remote Sensing Applications. Society and Environment.
Lourdes, L., Karina, Z., Pedro, L., Héctor, M., Néstor, M., 2011. A dynamic simulation model of land cover in the Dulce Creek Basin, Argentina. Procedia Environ. Sci. 7, 194–199.
McRae, B.H., Schumaker, N.H., McKane, R.B., Busing, R.T., Solomon, A.M., Burdick, C.A., 2008. A multi-model framework for simulating wildlife population response to land-use and climate change. Ecol. Model. 219 (1), 77–91.
Petz, K., Schulp, C.J., van der Zanden, E.H., Veerkamp, C., Schelhaas, M.J., Nabuurs, G.J., Hengeveld, G., 2016. Indicators and Modelling of Land Use, Land Management and Ecosystem Services: Methodological Documentation. PBL Netherlands Environmental Assessment Agency.
Pontius, R.G., Boersma, W., Castella, J.C., Clarke, K., de Nijs, T., Dietzel, C., et al., 2008. Comparing the input, output, and validation maps for several models of land change. Ann. Reg. Sci. 42 (1), 11–37.
Promper, C., Puissant, A., Malet, J.P., Glade, T., 2014. Analysis of land cover changes in the past and the future as contribution to landslide risk scenarios. Appl. Geogr. 53, 11–19.
Qiu, L., Zhu, J., Pan, Y., Hu, W., Amable, G.S., 2017. Multi-criteria land use suitability analysis for livestock development planning in Hangzhou metropolitan area, China. J. Clean. Prod. 161, 1011–1019.
Roy, P.S., Roy, A., Joshi, P.K., Kale, M.P., Srivastava, V.K., Srivastava, S.K., Dwevidi, R.S., Joshi, C., Behera, M.D., et al., 2015. Development of decadal (1985-1995-2005) land use and land cover database for India. Rem. Sens. 7, 2401e2430.
Saaty, T.L., 1980. The Analytic Hierarchy Process: Planning, Priority Setting, Resource Allocation. McGraw-Hill, New York.
Saaty, T.L., 2005. The analytic hierarchy and analytic network processes for the measurement of intangible criteria and for decision-making. In: Multiple Criteria Decision Analysis: State of the Art Surveys. Springer, New York, NY, pp. 345–405.
Sabia, G., De Gisi, S., Farina, R., 2016. Implementing a composite indicator approach for prioritizing activated sludge-based wastewater treatment plants at large spatial scale. Ecol. Indicat. 71, 1–18.
Sahoo, S., Dhar, A., Debsarkar, A., Kar, A., 2018. Impact of water demand on hydrological regime under climate and LULC change scenarios. Environ. Earth Sci. 77 (9), 341.
Saymohammadi, S., Zarafshani, K., Tavakoli, M., Mahdizadeh, H., Amiri, F., 2017. Prediction of climate change induced temperature & precipitation: the case of Iran. Sustainability 9 (1), 146.
Shukla, R., Khare, D., Deo, R., 2015. Statistical downscaling of climate change scenarios of rainfall and temperature over indira sagar canal command area in Madhya Pradesh, India. In: ICMLA, pp. 313–317.

Steiner, F., 2004. Commentary Philos. Geogr. 7 (1), 141–149. https://doi.org/10.1080/1090377042000196065.
Sun, X., Yue, T., Fan, Z., 2012. Scenarios of changes in the spatial pattern of land use in China. Procedia Environ. Sci. 13, 590–597.
Swets, J.A., 1988. Measuring the accuracy of diagnostic systems. Science 240 (4857), 1285–1293.
Verburg, P.H., Soepboer, W., Veldkamp, A., Limpiada, R., Espaldon, V., Mastura, S.S., 2002. Modeling the spatial dynamics of regional land use: the CLUE-S model. Environ. Manag. 30 (3), 391–405.
Yalew, S.G., van Griensven, A., Mul, M.L., van der Zaag, P., 2016. Land suitability analysis for agriculture in the Abbay basin using remote sensing, GIS and AHP techniques. Model. Earth Syst. Environ. 2 (2), 1–14.
Zhang, L., Nan, Z., Yu, W., Ge, Y., 2015. Modeling land-use and land-cover change and hydrological responses under consistent climate change scenarios in the Heihe River Basin, China. Water Resour. Manag. 29 (13), 4701–4717.
Zotarelli, L., Dukes, M.D., Romero, C.C., Migliaccio, K.W., Morgan, K.T., 2010. Step by Step Calculation of the Penman-monteith Evapotranspiration (FAO-56 Method). Institute of Food and Agricultural Sciences. University of Florida.